

## Preliminary Study of the GEM Detector Fringe Field Effect on the Accelerator Units

N. Martovetsky  
SSC Laboratory

June 22, 1992

Abstract:

The perpendicular component of the magnetic field has been evaluated in the forward direction along the beamline in the experimental hall of the GEM detector, taking into account ferromagnetic collimator and shield of the first quadrupole.

# PRELIMINARY STUDY OF THE GEM DETECTOR FRINGE FIELD EFFECT ON THE ACCELERATOR UNITS

N. Martovetsky  
June 22, 1992

## ABSTRACT

The perpendicular component of the magnetic field has been evaluated in the forward direction along the beamline in the experimental hall of the GEM detector, taking into account ferromagnetic collimator and shield of the first quadrupole.

## INTRODUCTION

The magnet for the GEM detector does not have neither iron return yoke nor an active shielding and allows relatively strong fringe field outside the magnet. The field flux density in the experimental hall is in the range 300 - 1000 G in the vicinity of Forward Field Shaper (FFS). The principle reason for an unshielded magnet concept is that it is easier to shield relatively small volumes of the elements which are sensitive to the magnetic field, than to shield huge volume of the detector magnet.

Stray field of the magnet is especially strong in the direction along the beam line, so it is necessary to evaluate the field effect produced by GEM fringe field on at least closest accelerator units - collimator and first quadrupole.

The objective of the study is to determine the value and distribution of the perpendicular component of the stray field on the beam due to the misalignment of the central line of the magnet relatively to the beam line.

## RESULTS AND DISCUSSION

Fig.1-6 shows field distribution in the forward area in front of the FFS assuming that there are no ferromagnetic elements in this area<sup>1</sup>. As may be expected in the area around beam line the field is mostly longitudinal, with small radial gradient of about  $5 \cdot 10^{-2}$  T/m

---

<sup>1</sup> J.Sullivan, private communication  
<sup>2</sup> N.Mokhov, private communication

at the most severe region near the FFS and an order of magnitude smaller gradient in the area of the quads location. Total field varies from 0.5 T to 0.04 T in the region of 18 to 36 m along the beam (0 denotes the Interaction Point). This implies that any iron component will be partially saturated in this area.

We developed a model shown in Fig. 7 to the collimator and the quadrupole with their ferromagnetic shields. Here, region 1 is the coil, region 5 is the FFS, region 7 is a collimator iron (i.d. 10 cm, o.d. 1 m) and region 10 is the return yoke of the accelerator quadrupole (i.d. 14 cm, o.d. - 34 cm). Length of collimator is taken to be 2 m, dipole shield is 15 m long<sup>2</sup>.

Location of the collimator is assumed to start at 19 m from the IP instead of 18m specified in accelerator - detector interface earlier because in present design, the FFS ends at 18 m and we assume that 1 m distance will be needed for the service.

The code used for analysis is PE2D.8. It allows for a 2D analysis, only, so we didn't take into account the field generated by quadrupole. In the first approximation, we can evaluate the radial field due to ferromagnetic elements off center of a symmetry line by comparing cases with ferromagnetic elements present and absent. This procedure allows to estimate the order of magnitude of the radial field in the beam region.

In Fig.8. are shown the flux lines in the forward direction. The main perturbation of the field occurs at the ends of the ferromagnetic elements. The field inside those elements is not significantly distorted in the radial direction.

Fig.9 supports this observation. It shows the radial component of the field (vertical axis, units are in Teslas, in contrast to previous drawings where units were in Gauss) for the case of 1 cm offset distance from the geometrical center of the magnet along the beam line. The main perturbations occur near the edges of ferromagnetic objects at about  $z= 10, 18, 19$  and  $21$  m, .

A measure of the influence of the radial component of the magnetic field on the beam is given by an integral of radial field along the beam calculated assuming offset from the magnet central line.

In Table 1 values of the integral  $\int B_r dz$  are shown for the axisymmetric configuration of the iron and for the case when iron is absent.

Table 1. Radial field in the beam vicinity

Range of integration	$\int B_r dz$ (1 cm offset from beamline), [T*m]	$\int B_r dz$ (2 cm offset from beamline), [T*m]
With iron of collimator and 1st quadrupole		
$z = 18+37$ m	0.0109	0.0105
$z = 0+37$ m	0.000247	-0.00991
With no iron in the forward direction		
$z = 18+37$ m	-0.00132	-0.00276
$z = 0+37$ m	-0.0123	-0.0240

As can be seen from the above table, the influence of the radial magnetic field is weak and not monotonous neither with increasing offset distance nor with the increasing integration length along the beam. Comparison of the  $\int B_r dz$  values for a path in the ranges  $z=18+37$  and  $z=0+37$  shows, that the average radial field acts in opposite directions inside the detector and in the FFS region. This further reduces the overall effect of radial field on the beam.

For the 2 cm beam offset distance, the average integrated radial field in this region is equal to 2.68 G.

In Table 1 are shown also the values of the integral for the case with no iron in the vicinity of the beam line.

## CONCLUSION

The computation of the radial component of the magnetic field on the beam has been performed, using axisymmetric 2d model and taking into account the ferromagnetic elements of the beam transport units and possible misalignment of the magnetic center relatively to the beam line. It is shown, that the average transversal (radial) component of the field is of an order of few Gauss. The results demonstrate that in the region of 0-37 m beam line iron elements reduce the effect of the radial field and allow to use the iron free forward area calculations as a conservative approach.

CEM Case 511: Res 0.5m  
Gap 1.5m  
MITMAP SV 18.0 Wed 3/24/00 (0m, 18m) 13:55  
Variable Contour Increments

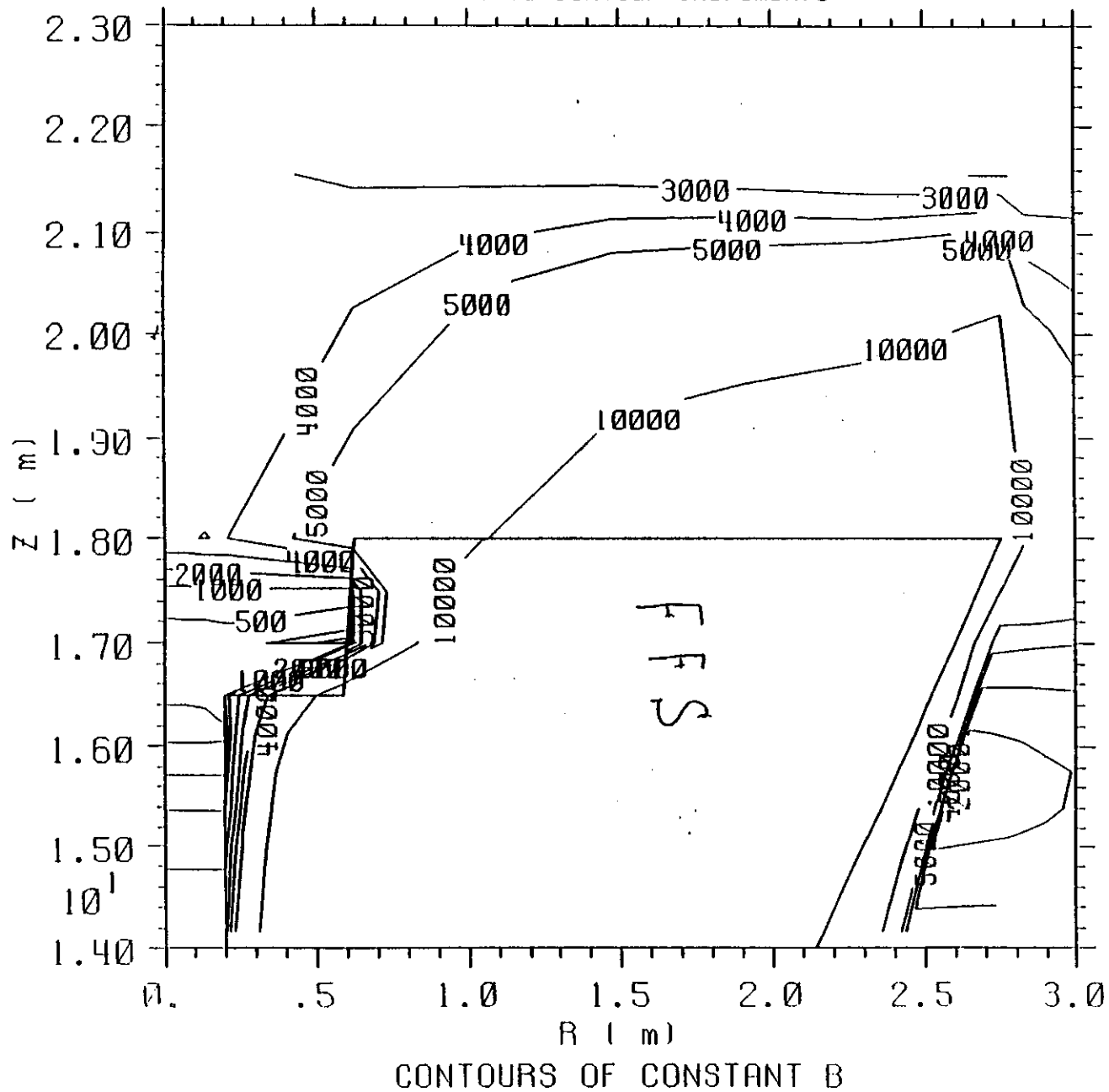
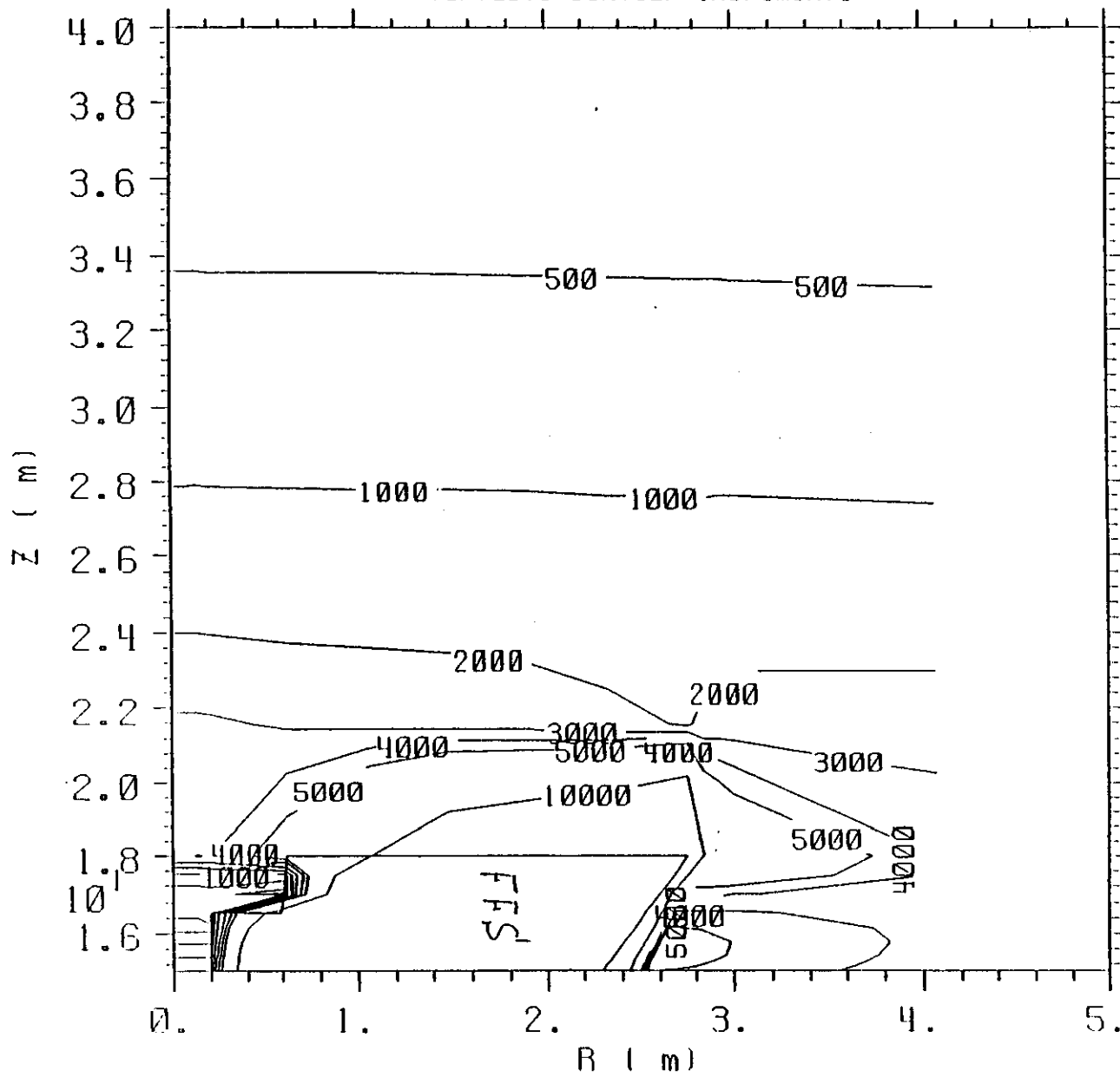


Fig 1

CEM Case 511: Res 0.5m  
Gap 1.5m  
MITMAP SV 18.0 Wed 3/24/00 (m, 18m) 13:53  
Variable Contour Increments



CONTOURS OF CONSTANT B

Fig. 2

SEM Case 511: Rod 0.5m  
Gap 1.5m  
MITMAP SV18.0 deg/24 (0m, 18m).13:54  
Variable Contour Increments

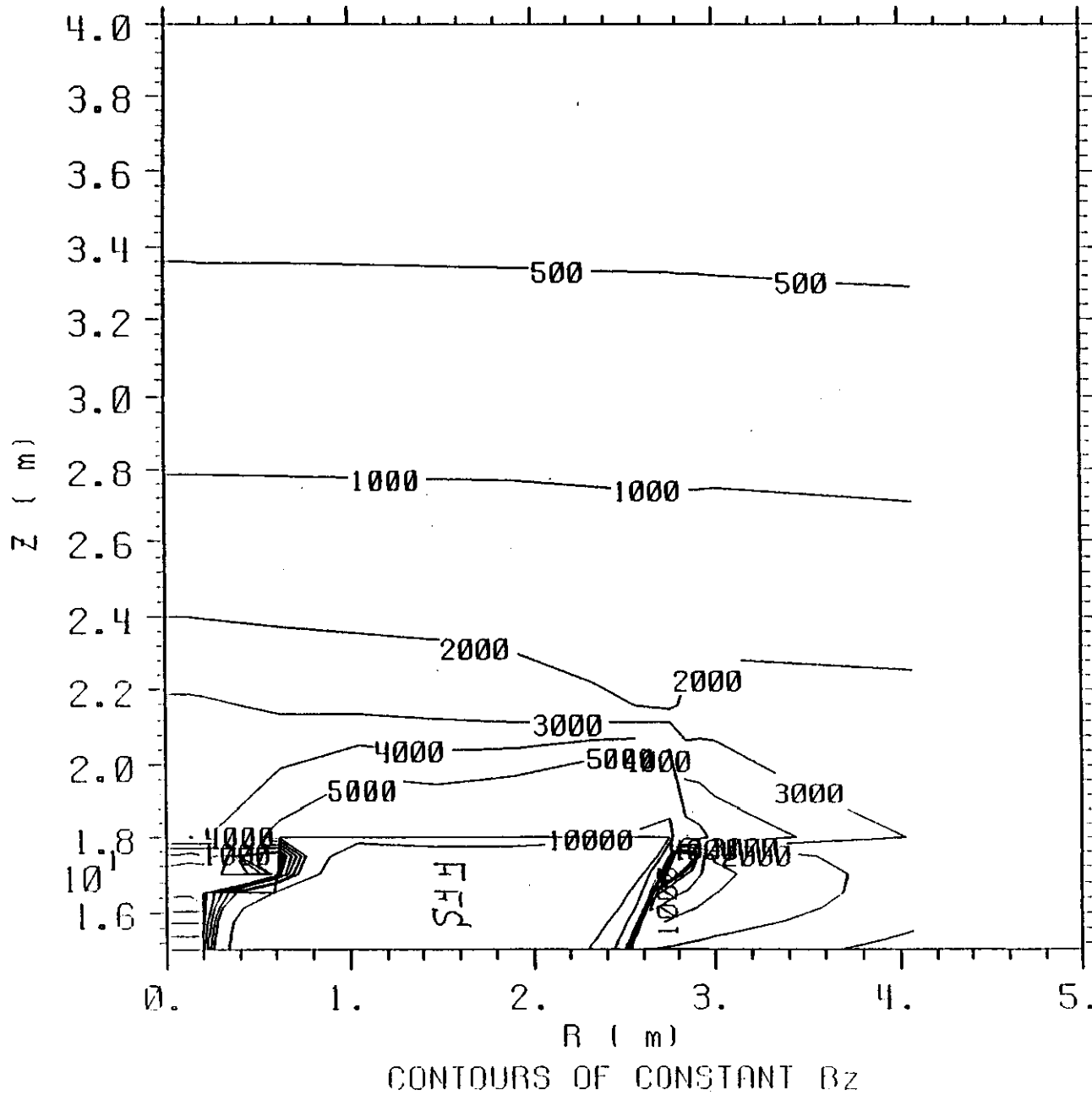


Fig. 2

CEM Case 511: Rad 0.5m  
Gap 1.5m  
MITMAIP SV 18.0 Wed 3/24/00 (m. 18m). 13:54  
Variable Contour Increments

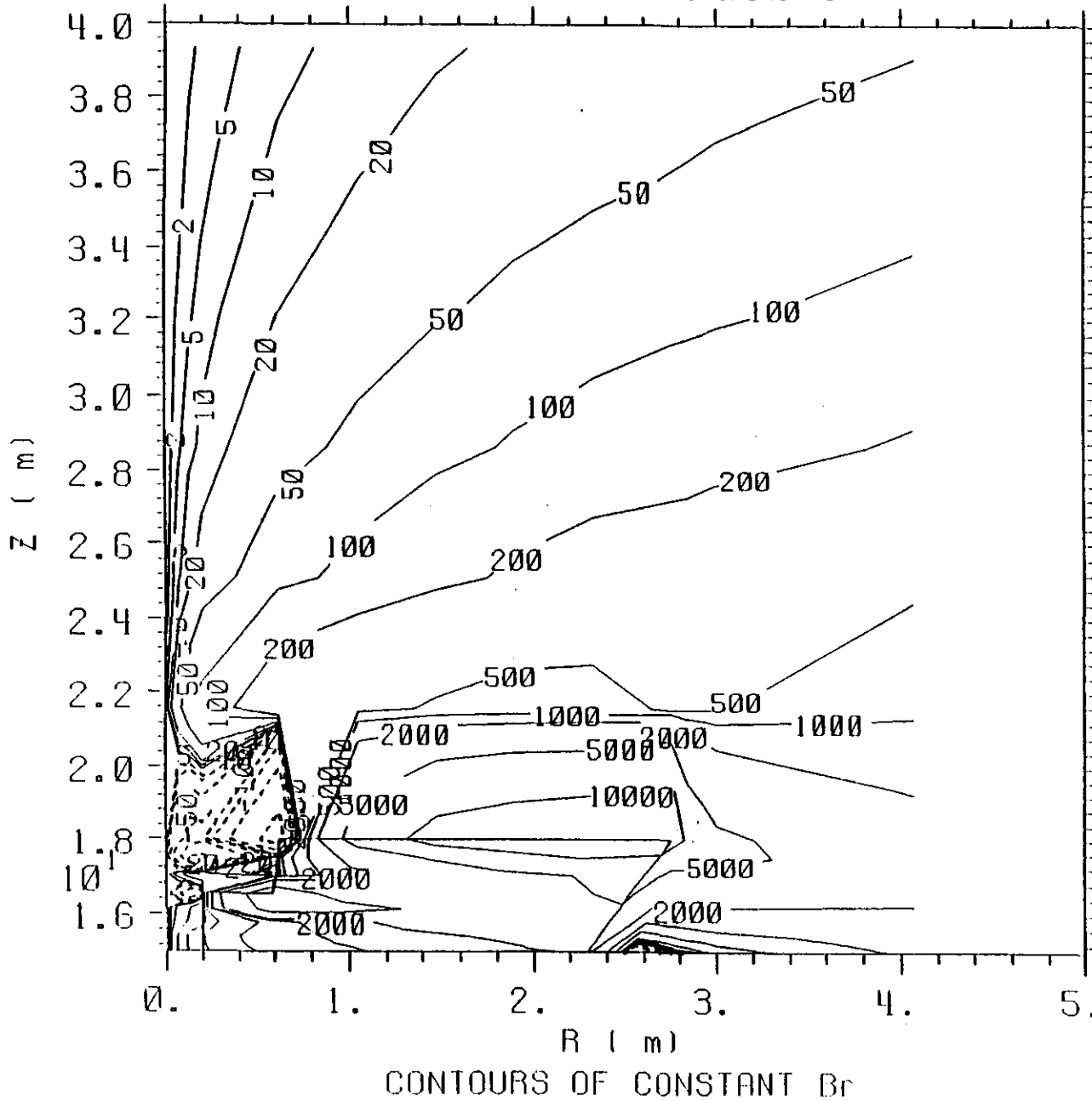


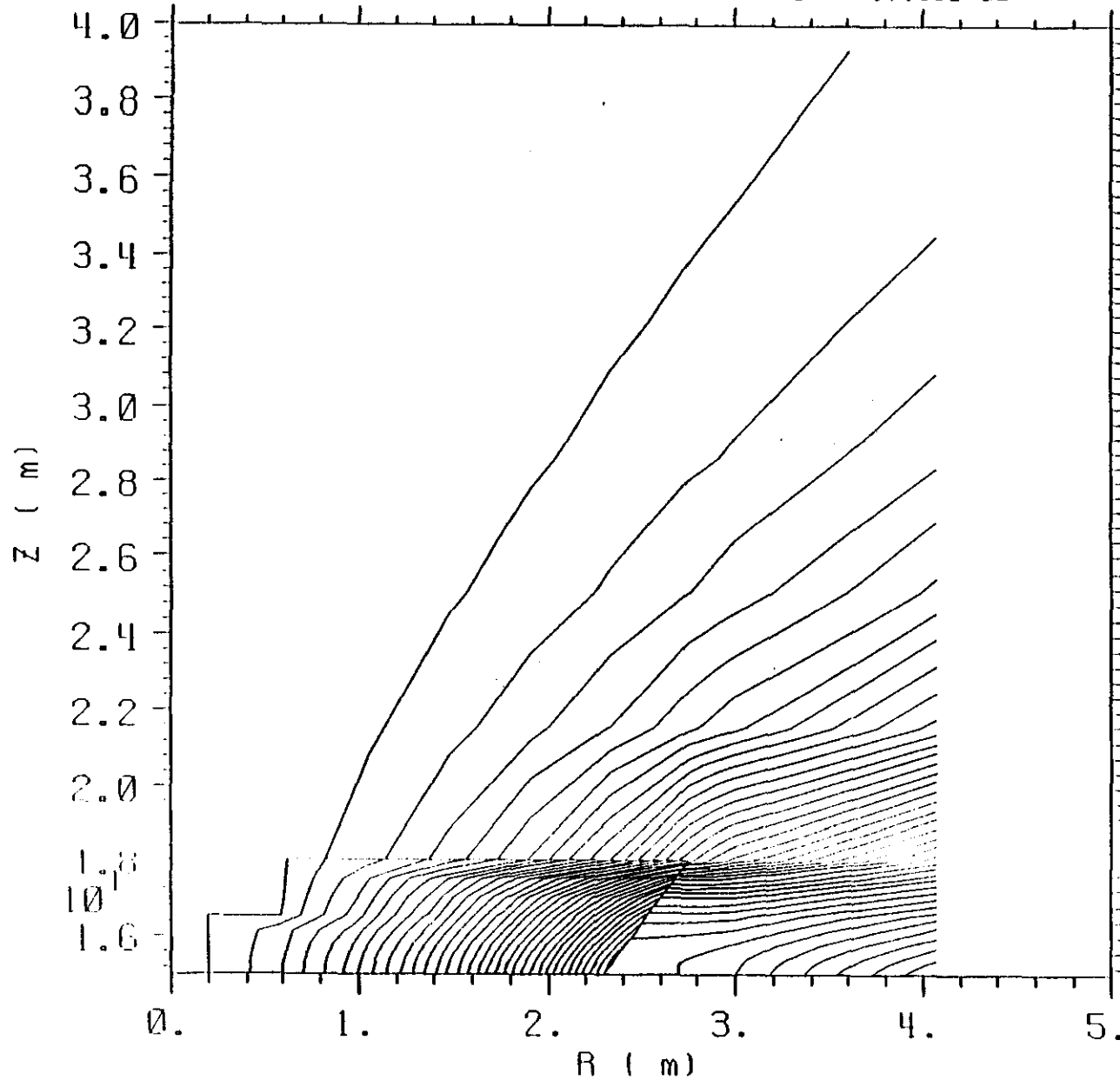
Fig 4

SEM Case 511: Rsc 9.5m

Gap 1.5m

MITMAP SV 18.0 deg / 21 / 00 (m. 18m) 13:55

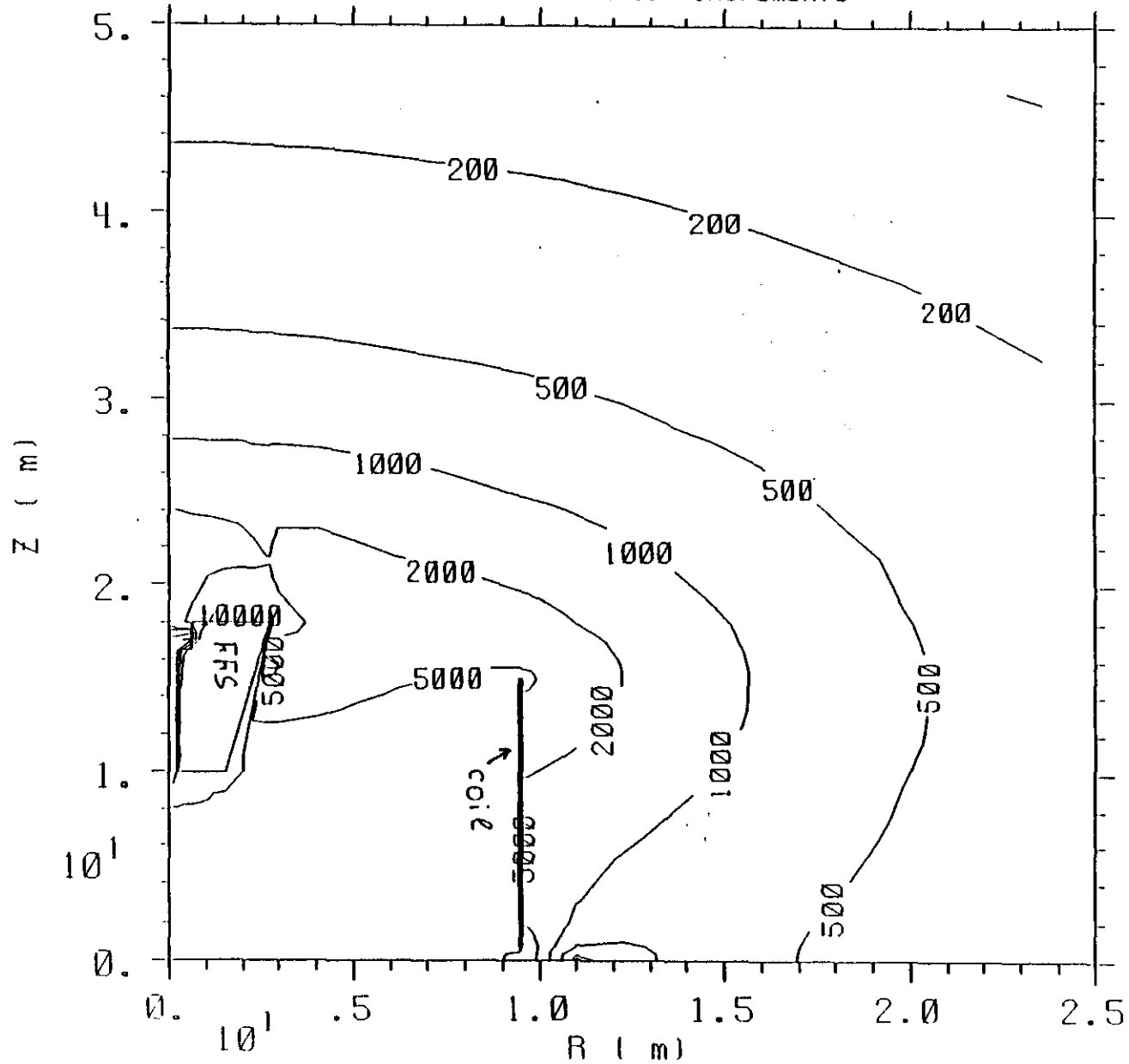
Contour 1 = 0.000E+00 Delta = 1.166E+00



CONTOURS OF CONSTANT FLUX

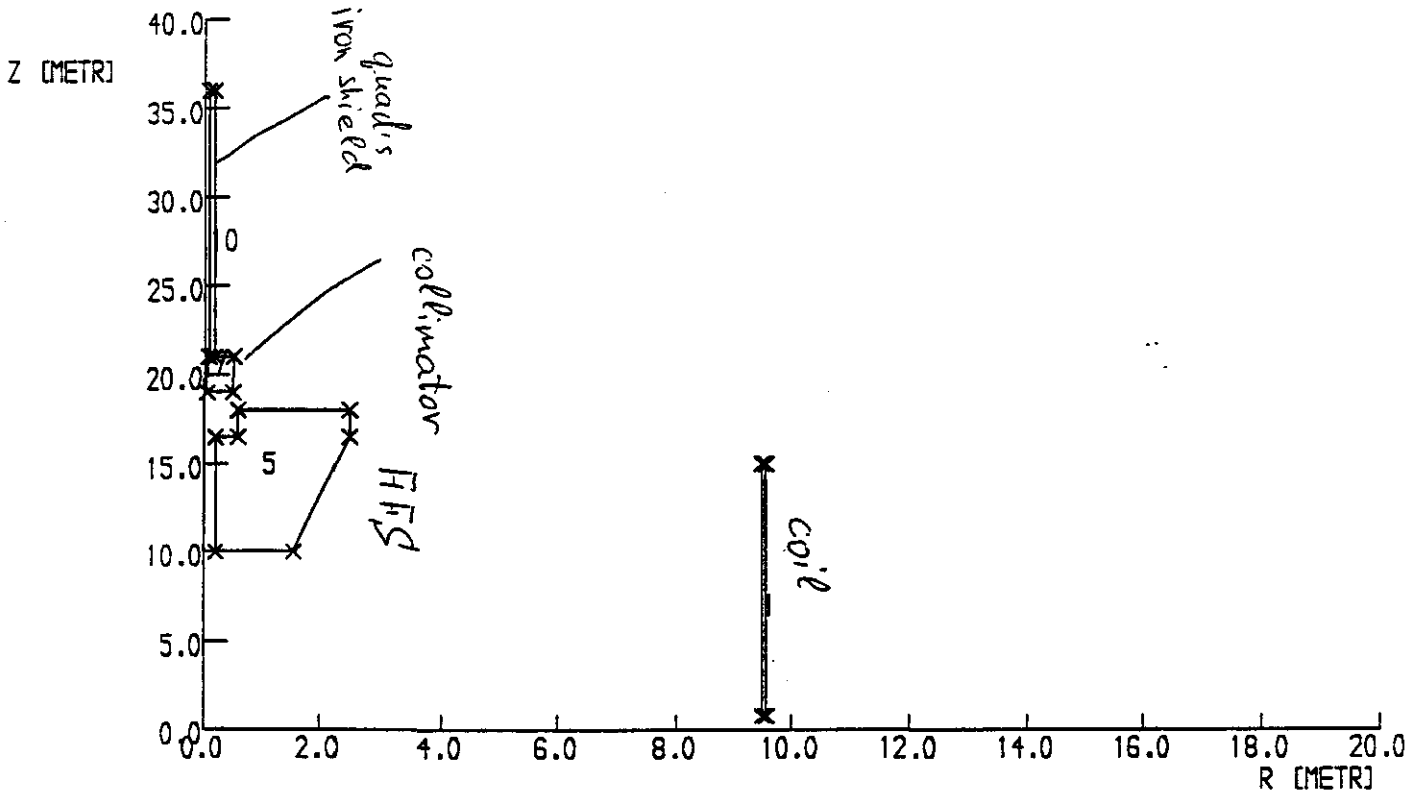
Fig. 5

SEM Case 511: Rod 0.5m  
Gap 1.5m  
MITMAPSV18.0 deg/24/00 (m. 18m) 13:56  
Variable Contour Increments



CONTOURS OF CONSTANT R

Fig. 6



ELEM=QUAD SYMM=AXI SOLN=AXI SCALE=1.0 FIEL=MAGN  
Static Solution Mesh 3369 Elements 11 Regions

VF/PE2D.8

Fig. 7

GEMFSSIM.STRES  
18/Jun/92 08:08:28

Page 4 . AUTO STAR=3.00 FI=0.05 LAB=ER

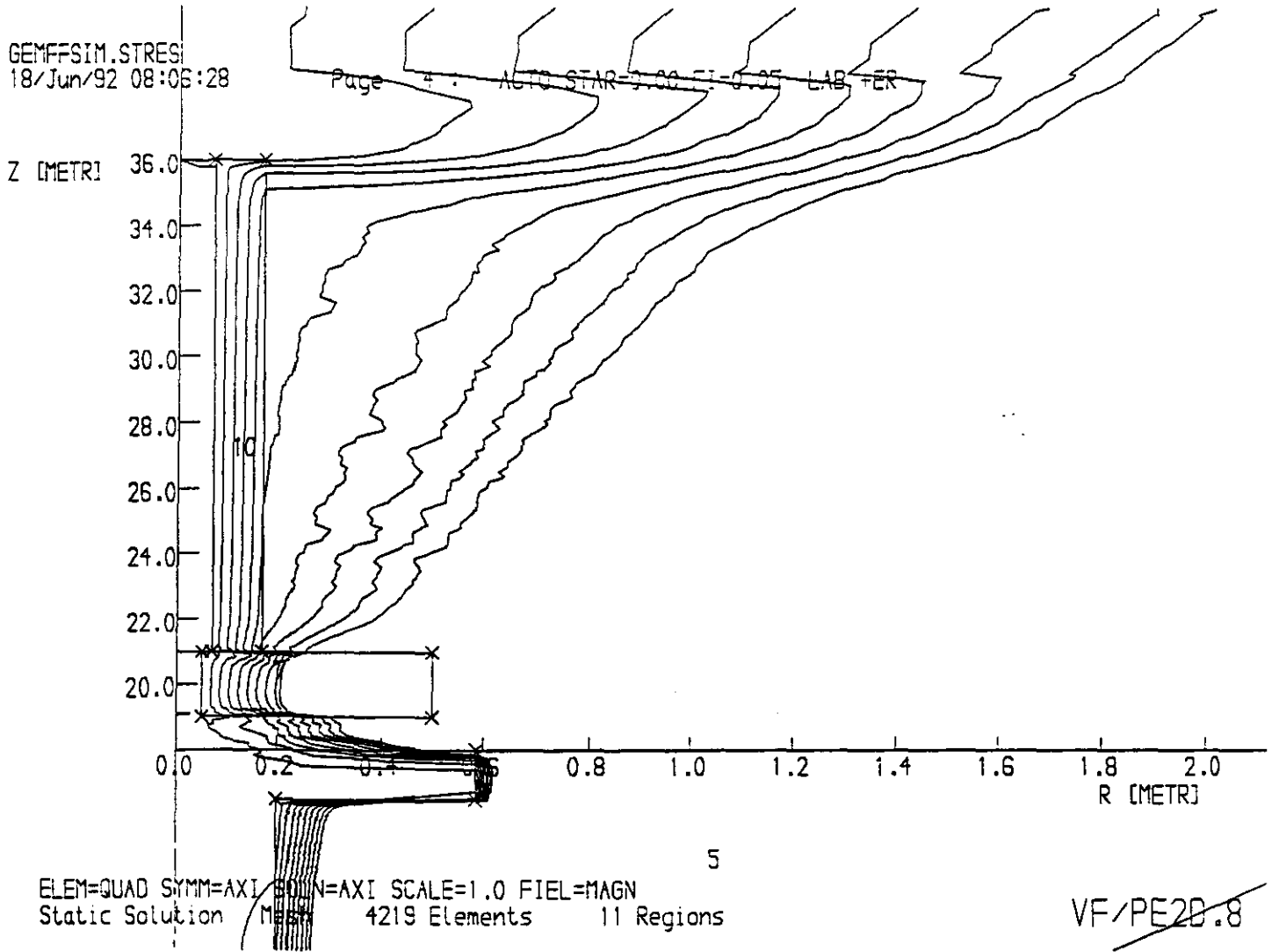
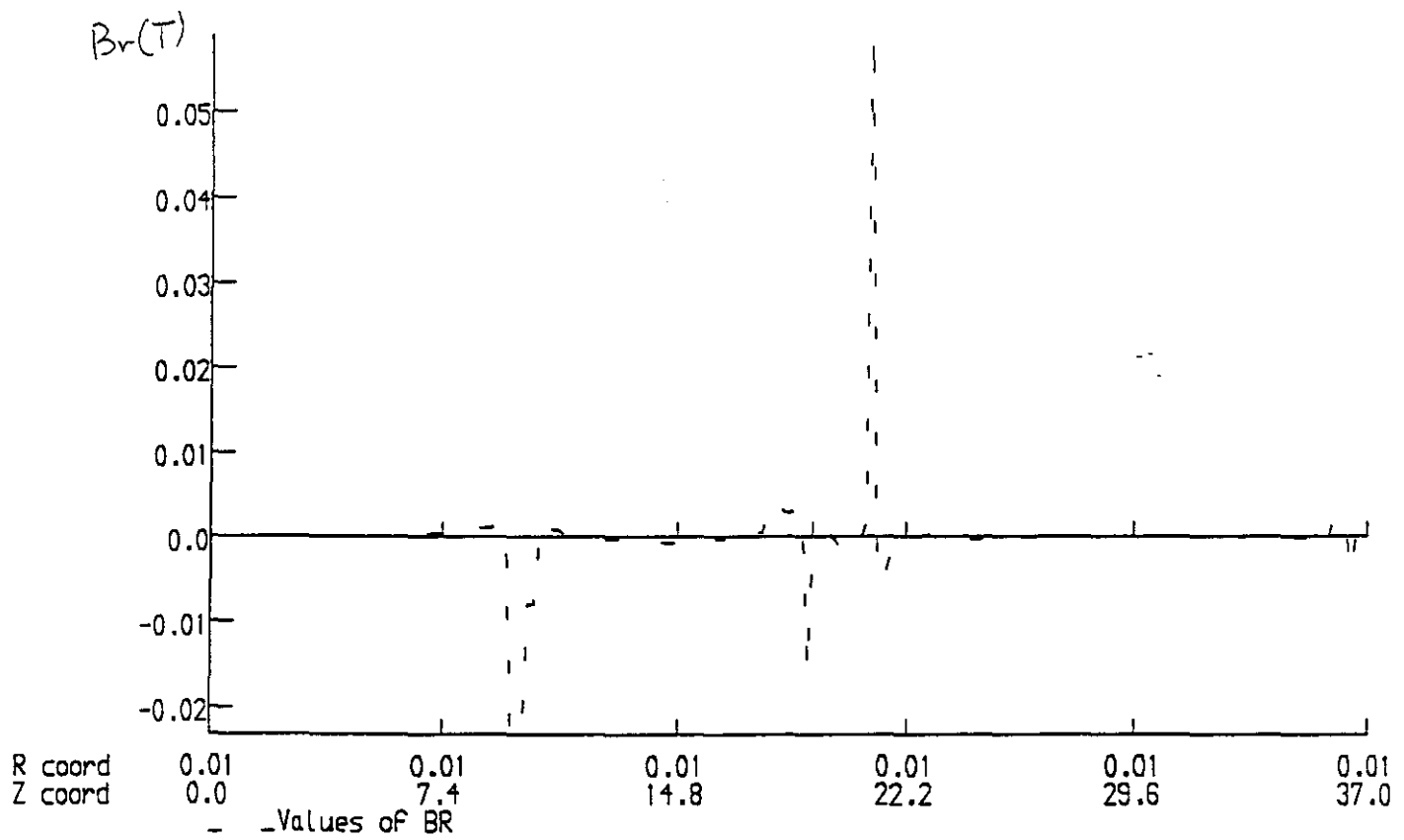


Fig. 8



VF/PE2D.8

Fig. 9